CHAPTER VI

DIELECTRIC STUDY OF MATERIALS EXHIBITING CRYSTAL B AND HEXATIC B PHASES

6.1 INTRODUCTION

The smectic B liquid crystalline phase is a layered phase with molecules oriented perpendicular to the layer planes and ordered hexagonally within each layer. Recent high resolution Xray studies[1] have demonstrated that this hexagonal order in the liquid crystal n-(4-n-butyloxybenzylidene)-4-n-octylaniline (40.8), a prototype material exhibiting B phase, involves positional correlations which are three dimensional (3D) and long-range. It was observed that in this material the in-planar ordering extended over at least 14000 Å and limited by the resolution of the set up.[1] This smectic B phase is therefore now referred to as crystalline B phase. We shall be abbreviating this as B_{cryst} in this chapter. This B phase supports a shear both within and between its layers and melts when heated into the smectic A phase – a phase that is fluid with regard to the in-plane ordering. Although many of the observed B phases appeared to be B_{cryst} phases, Leadbetter et al.[2] argued that some materials exhibiting B phases appeared to lack interlayer correlations.

Halperin and Nelson[3] first proposed the possibility of bond-orientational ordering in their treatment of two-dimensional (2D) melting. They found that a 2D phase having algebraically decaying bond-orientational order (a hexatic phase) could exist between the 2D solid and liquid phases if 2D melting was a dislocation-mediated second order phase transition. Subsequently, Birgeneau and Litster[4] suggested the existence of a 3D liquid crystal phase consisting of 2D hexatic layers which interact to produce long-range, 3D bond-orientational order. Xray studies performed by Pindak et al.[5] on free-standing films of n-hexyl-4'-pentyloxybiphenyl-4-carboxylate (65OBC) led to the discovery of such a B phase having short-range in-plane positional correlations but long-range, three dimensional, sixfold bond-orientational order. This new phase is now generally referred to as hexatic B phase (B_{hex}). Since the discovery of this phase in 65OBC, several other materials have been synthesised which are known to exhibit srnectic A-B_{hex} phase transition, one of them being n-butyl-4'-hexyloxybiphenyl-4-carboxylate (46OBC). Extensive high resolution heat capacity measurements[6-11] were carried out near A-B_{hex} transition of various materials. It has been observed that the critical exponent α characterising heat-capacity anomaly of A-B_{hex} transition is found to be large and does not vary systematically with the range of the smectic A phase. It was found that the value of α is in the range of 0.5 - 0.6 for all substances. There have also been several other experimental as well as theoreti-

cal studies of $A-B_{hex}$ transitions, e.g., the measurements of birefringence,[12] shear mechanical properties,[13] density[1,] and the analysis of the theoretical model[15] based on coupling between bond-orientational order and herring bone order.

We saw in chapter III that the dielectric behaviour of polar A materials is influenced by structural changes (as seen in Xray diffraction experiments[16,17]) occurring in the system. It is therefore of interest to make detailed dielectric studies of materials exhibiting two types of A-B transitions, viz., $A-B_{cryst}$ and $A-B_{hex}$ in order to compare and contrast their dielectric behaviour. With this in view, we have carried out a detailed dielectric study of $A-B_{cryst}$ transition in 40.8 and $A-B_{hex}$ transitions in 65OBC and 46OBC.

6.2 MATERIALS

The structural formulae of the materials are shown in Fig.6.1 and the sequences and temperatures of transitions are given in Table 6.1. All the transitions were identified by optical microscopy. The $A-B_{cryst}$ transition was identified from the transition bars seen on focal conics while the signature of the $B_{hex}-A$ transition was the **wishbones** texture.[18] The transition temperatures agree with those reported in the literature.[1,8] The dielectric measurements were carried out using the apparatus described earlier. A most difficult aspect of the experiment was to obtain perfectly aligned samples in the homeotropic and homogeneous geometries. A combina-

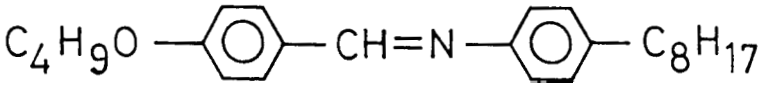

n-(4-n-butyloxybenzylidene)-4-n-octylaniline

(40.8)

2.

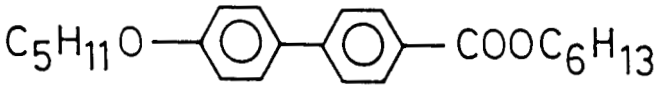

n-hexyl-4'-pentyloxybiphenyl-4-carboxylate

(650BC)

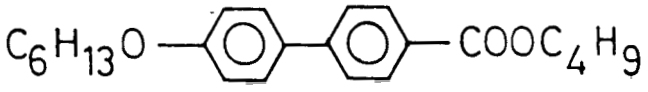

n-butyl-4'-hexyloxybiphenyl-4-carboxylate

(460BC)

Figure 6.1

The structural formulae and the abbreviations used for the compounds studied.

TABLE 6.1

The sequences and the temperatures of transitions of the compounds studied. (The temperatures are in degree celsius)

S. No.	Compound	Transition temperatures (in °C)
1	4O.8	I **78.9** → N **62.8** → A **48.2** → Crystal B
2	65OBC	I **83.6** → A **66.9** → Hexatic B **60.2** → E
3	46OBC	I **91.6** → A **66.8** → Hexatic B

tion of silane coating (octadecyl triethoxy silane) and 2.4T magnetic field was used for obtaining homeotropically aligned smectic A phase by slowly cooling from the isotropic phase (1°C/hr). The aligned A phase was then cooled to B phase at even slower rates to ensure that the alignment was not lost. The homogeneous alignment was obtained with the magnetic field only.

6.3 RESULTS AND DISCUSSION

6.3.1. **Static**

The variation of the static dielectric constants $\varepsilon_{\parallel}$ and $\varepsilon_{\perp}$ in different phases of 40.8 is shown in the figure 6.2. $\varepsilon_{\perp}$ is greater than $\varepsilon_{\parallel}$ in all the phases, i.e., the material exhibits negative dielectric anisotropy $\Delta\varepsilon$ throughout. Starting from the nematic phase, with decrease in temperature, $\varepsilon_{\perp}$ shows an increase while $\varepsilon_{\parallel}$ a decrease. At the N-A transition the increasing trend of $\varepsilon_{\perp}$ continues while $\varepsilon_{\parallel}$ shows a still steeper variation. The variation of $\varepsilon_{\parallel}$ in the A phase is greater than that in the nematic phase while that of $\varepsilon_{\perp}$ in A and N phases is essentially continuous. At the A-B_{cryst} transition, $\varepsilon_{\perp}$ increases while $\varepsilon_{\parallel}$ decreases and finally in the B_{cryst} phase both $\varepsilon_{\perp}$ and $\varepsilon_{\parallel}$ show a slight increase with decrease in temperature. The temperature variation of $\Delta\varepsilon$ is shown in the Fig. 6.3a. It is clear that there is a sudden jump in $\Delta\varepsilon$ at the A-B_{cryst} transition while there is only a smooth change of slope at the A-N transition.

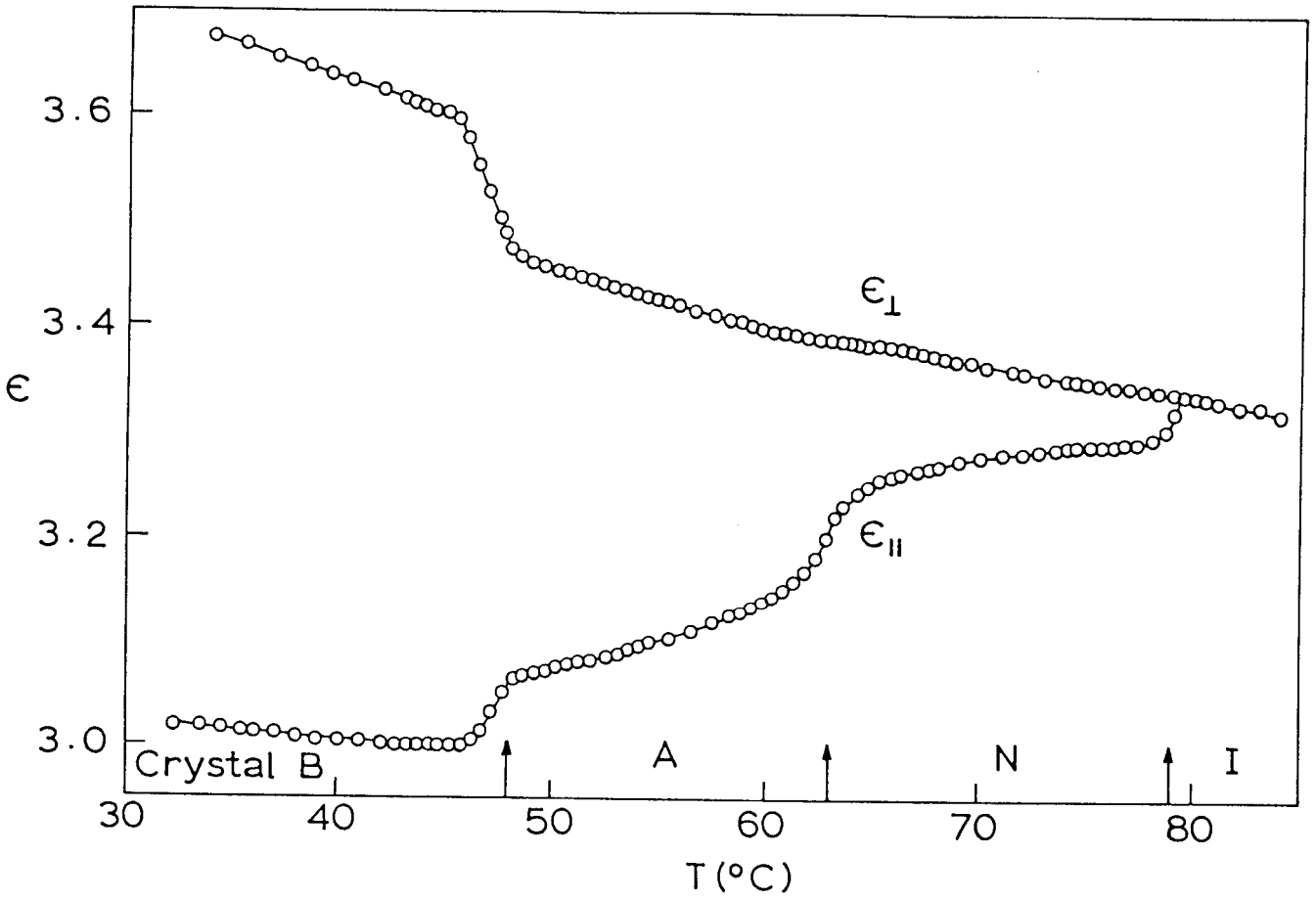

Figure 6.2

Variation of the static dielectric constants $\epsilon_\parallel$ and $\epsilon_\perp$ with temperature in the different phases of 40.8.

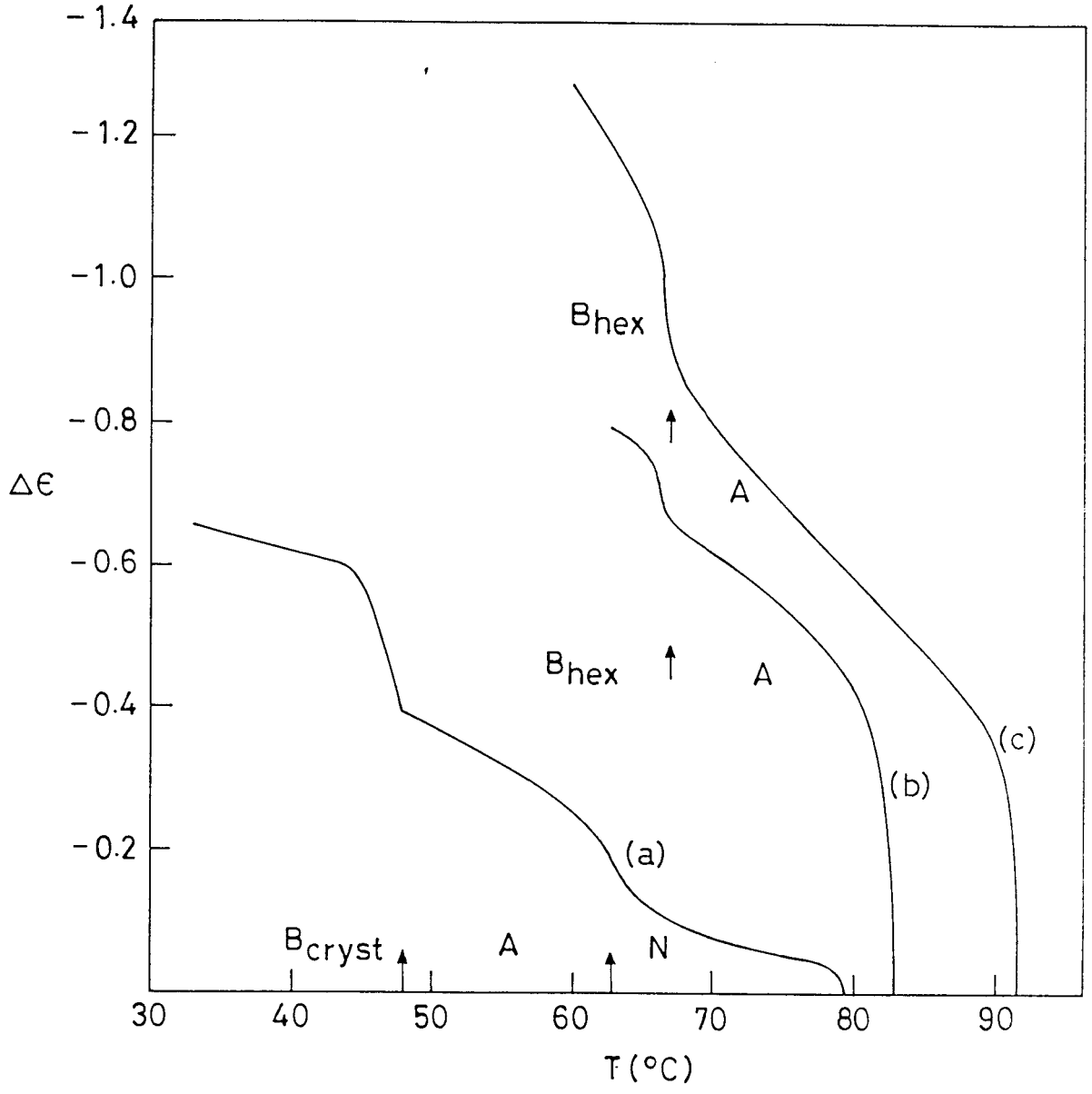

Figure 6.3

The temperature variation of the dielectric anisotropy Δε of (a) 40.8, (b) 650BC and (c) 460BC.

The temperature variation of static dielectric constants of 65OBC and 46OBC are shown in Figs. 6.4 and 6.5 respectively. Since both these materials do not show the nematic (N) phase, it was necessary to cool the sample from isotropic phase very slowly in the presence of the magnetic field in order to obtain the aligned A phase. The trends of temperature variation of $\varepsilon_{\parallel}$ and $\varepsilon_{\perp}$ of 65OBC are essentially similar to those of 46OBC. In the A phase, $\varepsilon_{\perp}$ shows an increasing trend with decrease in temperature while $\varepsilon_{\parallel}$ shows a decrease. At the A-B_{hex} transition, $\varepsilon_{\perp}$ increases slightly while $\varepsilon_{\parallel}$ decreases. The temperature variation of $\Delta\varepsilon$ for the two materials is shown in Fig. 6.3b &c. It is interesting to note that in all the three cases there is an increase in $\Delta\varepsilon$ at the A-B transition regardless of whether B phase is crystalline or hexatic. It is also interesting to note that $\varepsilon_{\perp}$ shows an increase on going from A to B_{hex} or B_{cryst} phase which can be interpreted as an increase in the hindrance to the molecular rotation in the more ordered B phase. We shall discuss this aspect in greater detail while discussing dispersion results.

Before presenting the dispersion results, we shall first discuss here the state of knowledge on the Xray studies of A-B_{cryst} in 40.8 and A-B_{hex} transition in 65OBC and 46OBC. This information is relevant to correlate the dielectric behaviour with the structural differences.

The A - B_{cryst} transition in 40.8 has been extensively studied

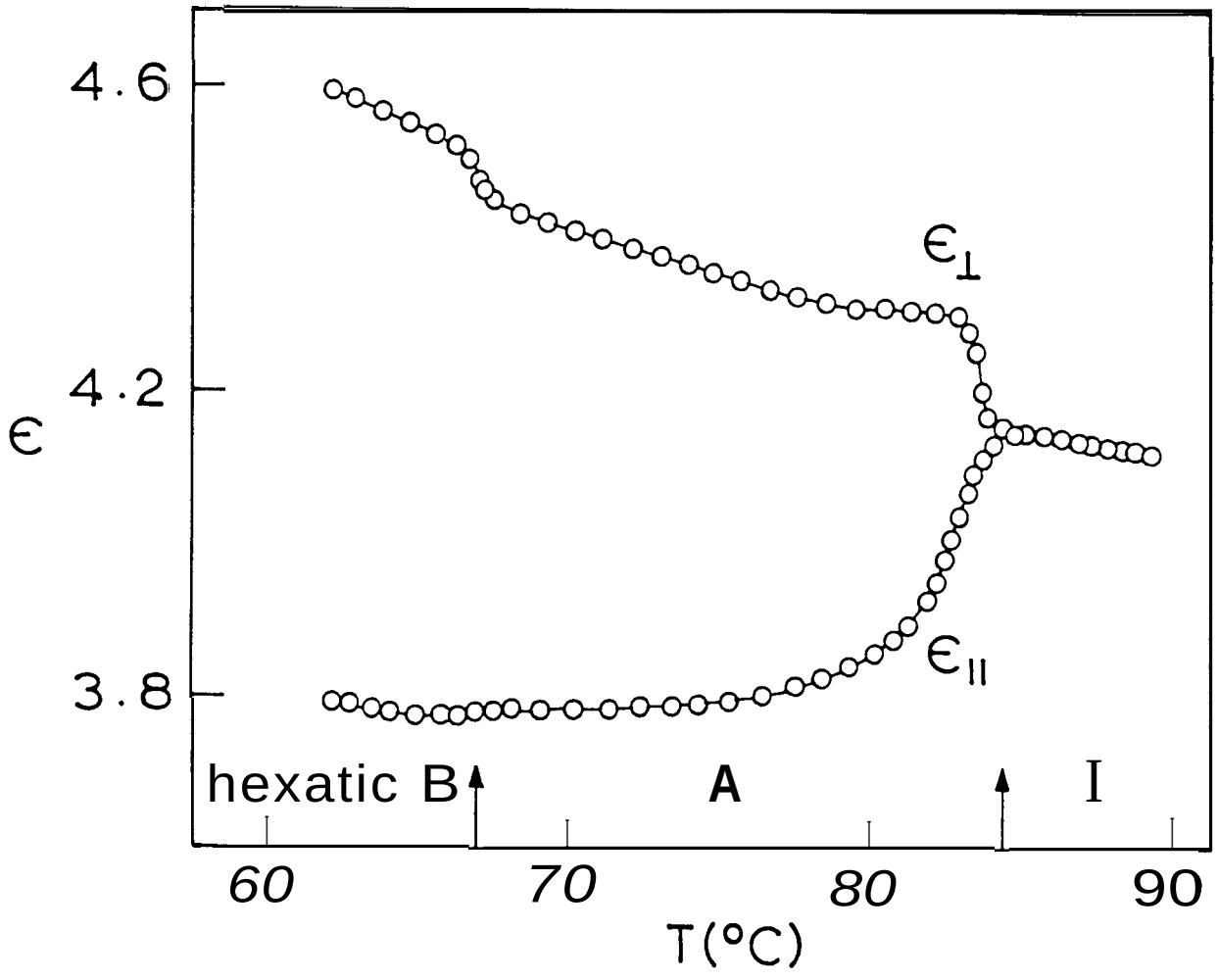

Figure 6.4

Variation of $\varepsilon_{||}$ and $\varepsilon_{\perp}$ with temperature in the different phases of 650BC.

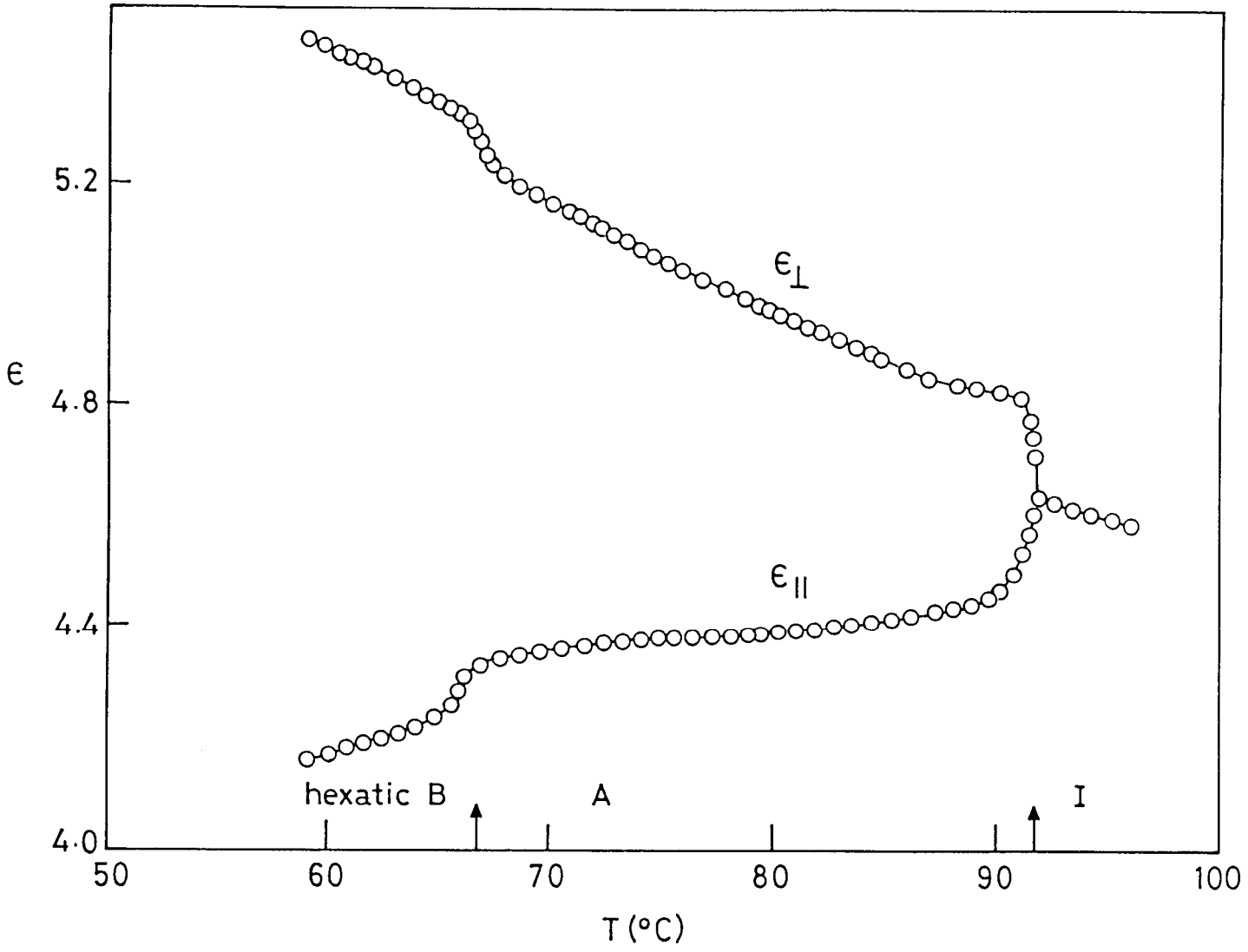

Figure 6.5

The temperature variation of $\epsilon_{||}$ and $\epsilon_\perp$ in the different phases of 460BC

using high resolution Xray technique by Pershan et al.[1] Two important results arising from the investigations are: (1) the in-planar correlation length in B_{cryst} phase is very large — greater than 14000 Å (resolution limited) and (ii) A-B_{cryst} transition is clearly first order with a small co-existence region which is characterised by the existence of the density modulations corresponding to both the A and B_{cryst} phases although difference between them was only about 1.3%. Fig.6.6 shows the Xray diffraction scan showing clearly co-existing density modulations in the two phase region of A-B_{cryst} transition. As mentioned earlier Xray studies on A-B_{hex} transition in 65OBC have been conducted by Pindak et al.[5] using free-standing film. They observed that in the vicinity of A-B_{hex} transition, there is a rapid increase in $\xi_{\|}$, i.e., in-plane positional correlation length measured along the director, from about 20 Å in A phase to 60 Å in B_{hex} phase. However $\xi_{\|}$ did not diverge at the phase transition (see Fig.6.7). Pindak et al. concluded that the positional ordering is not a relevant order parameter for A-B_{hex} transition. The important result from the experiments of Pindak et al.[5] is the observation of Xray scattering due to hexagonal bond-orientational correlations which are three dimensionally ordered.

The high resolution heat capacity measurements[6-9,11] carried out on 65OBC as well as 46OBC showed that A-B_{hex} transitions in both cases are second order with critical exponents of about

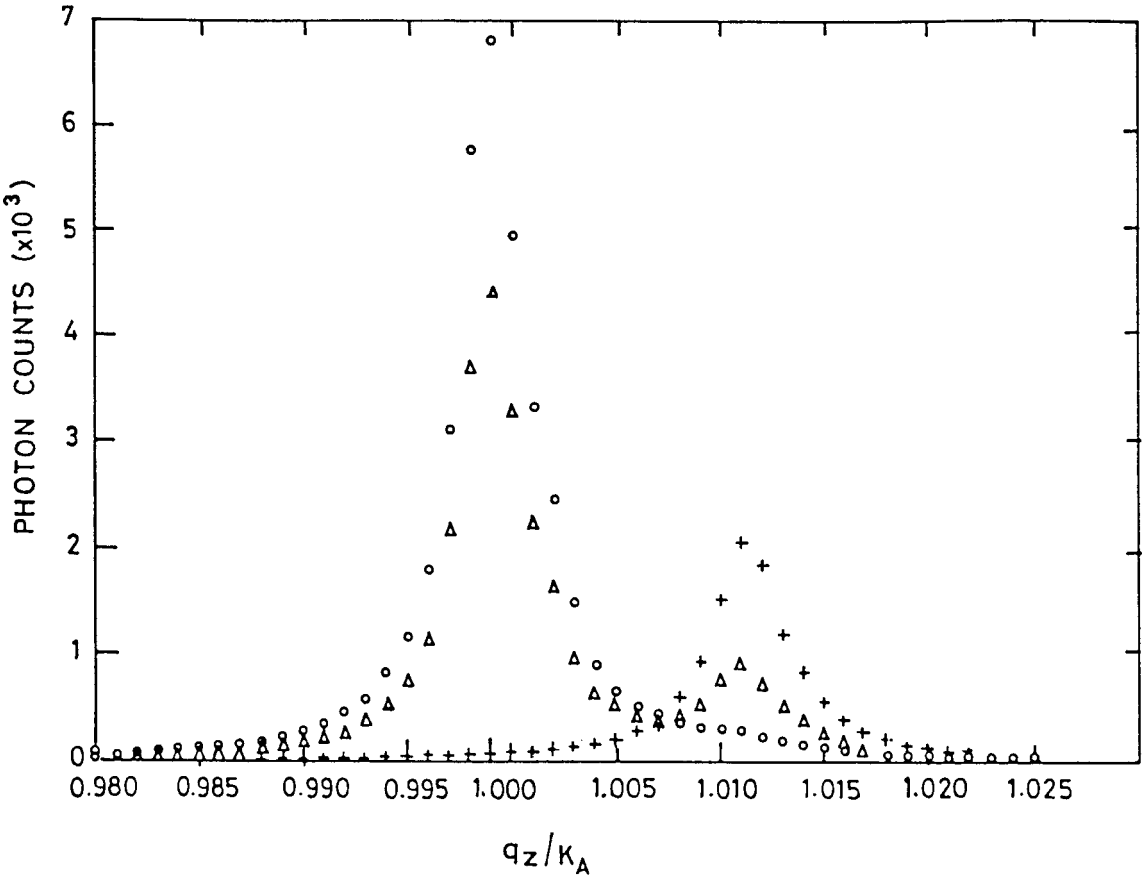

Figure 6.6

(0,0,1 - q_Z/K_A) scans at temperatures T = 49.3°C (smectic A phase) (+), T = 48.9°C (coexistence region) Δ, and T = 48.7°C (solid B phase) o (Ref. 1).

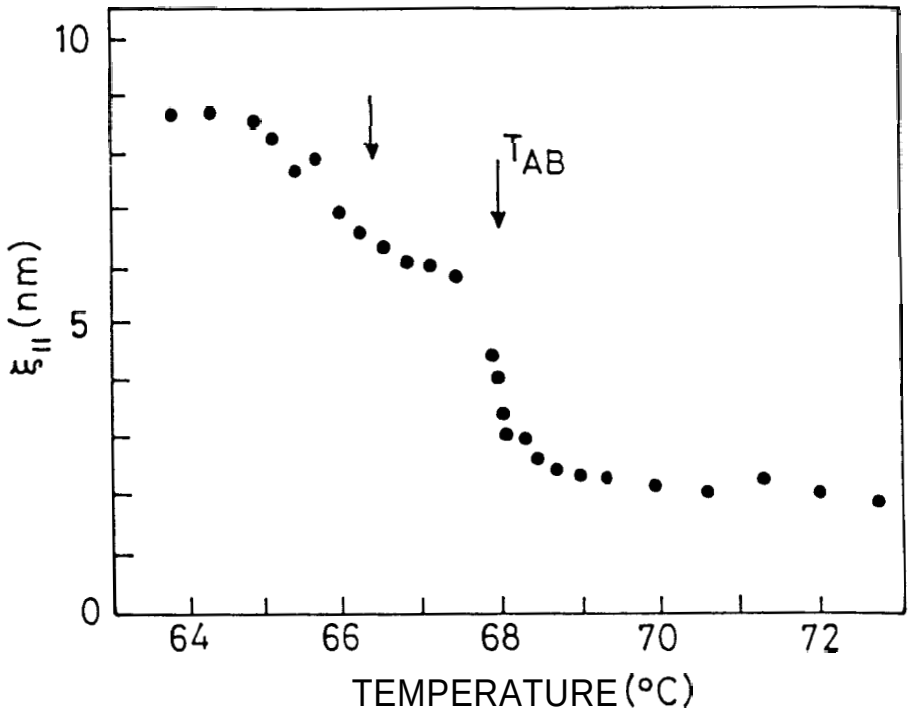

Figure 6.7

Temperature dependence of the in-plane positional correlation length $\xi_{\parallel}$ (Ref. 5).

0.6 and 0.49 respectively. The origin of this large critical exponent has not yet been understood and it is also not clear to which universality class the A-B_{hex} transition should belong. The accurate layer spacing measurements have been conducted by Geetha Nair[19] near A-B_{hex} transition of 65OBC and 46OBC. These data are given in Figures 6.8 and 6.9. The feature of the result was that no abrupt jump in the layer spacing was observed near A-B_{hex} transition in either of the two cases. Also no broadening of diffraction maxima was seen either at the A-B_{hex} transition in 65OBC or 46OBC. This can be compared with the data on 40.8 (see Fig.6.10) wherein a small jump in d was seen at the A-B_{cryst} transition accompanied by a broadening of the diffraction peak due to the co-existence of the density modulations of the A and B_{cryst} phases. It is interesting that although the changes in the in-plane positional ordering accompanying the A-B_{cryst} and A-B_{hex} transitions are drastically different,[1,5] there is hardly any significant difference in the variation of layer spacing d at the two transitions. With these results in the background, we shall describe the dispersion results.

6.3.2. **Dispersion**

The frequency of relaxation of $\varepsilon_{\parallel}$ (f_R) has been measured in A and B phases of all the three compounds. Special care was taken to acquire data at close intervals of temperature (−250 mK) in the neighbourhood of the transition in order to see if the first

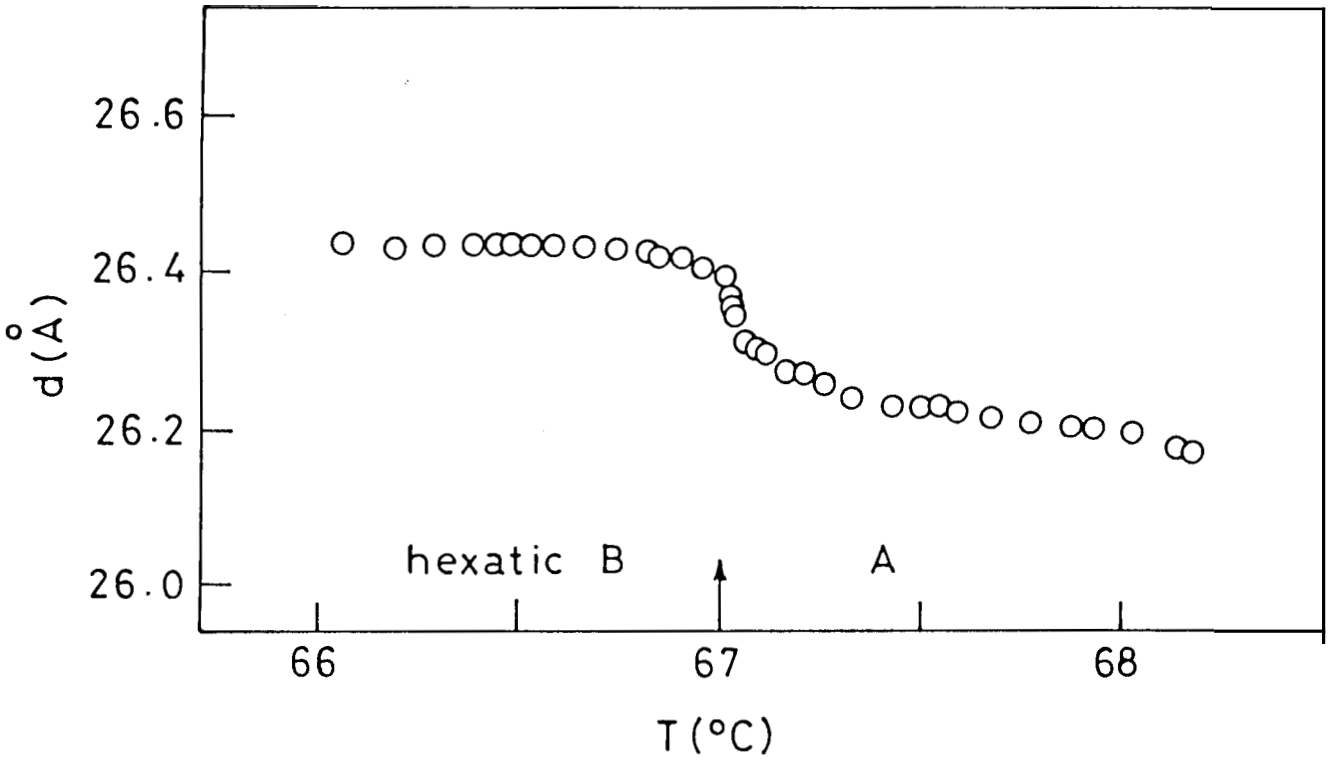

Figure 6.8

Variation of with temperature in the vicinity of the B_{hex} - A transition in 5OBC (Ref.19).

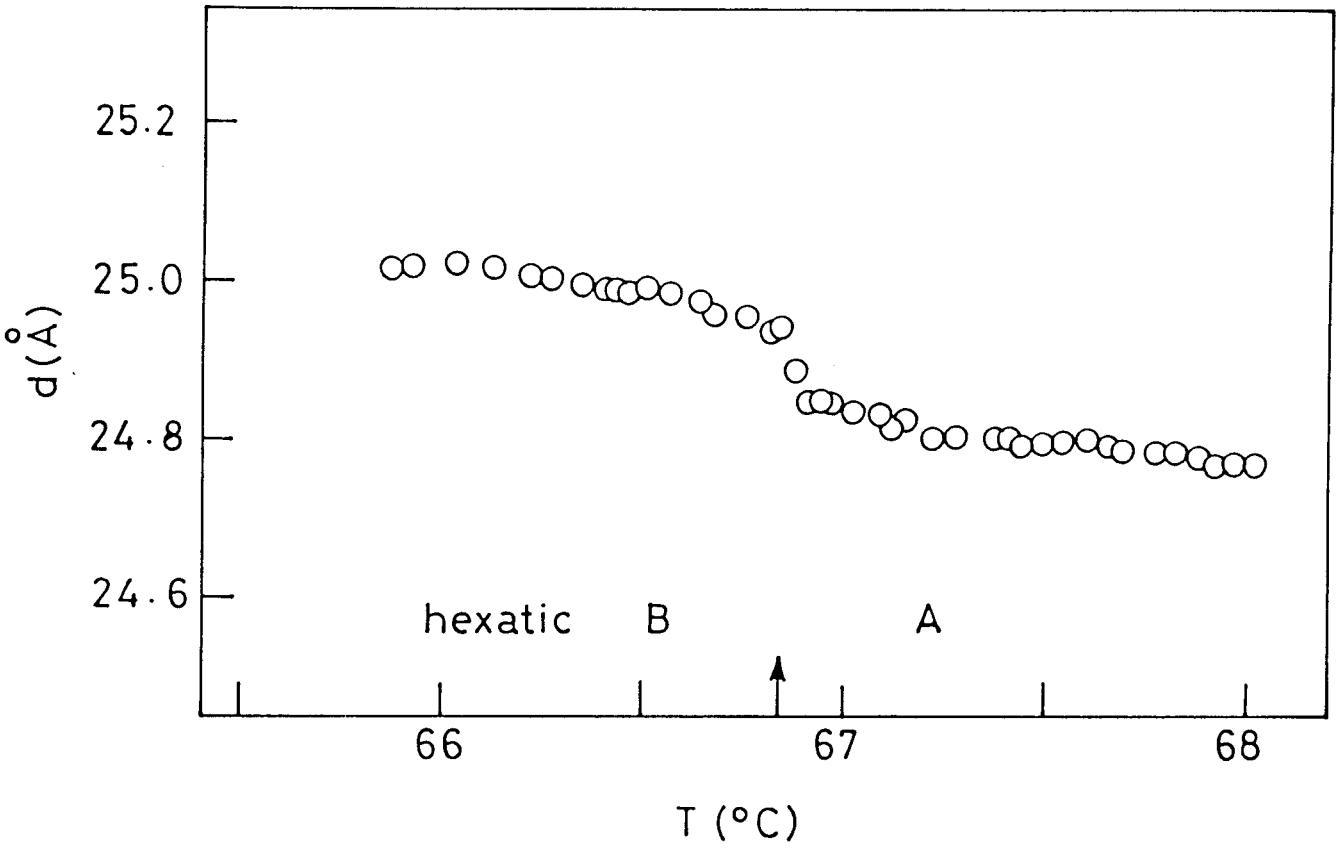

Figure 6.9

Variation of with temperature in the vicinity of the B_{hex} - A transition in 6OBC Ref.19).

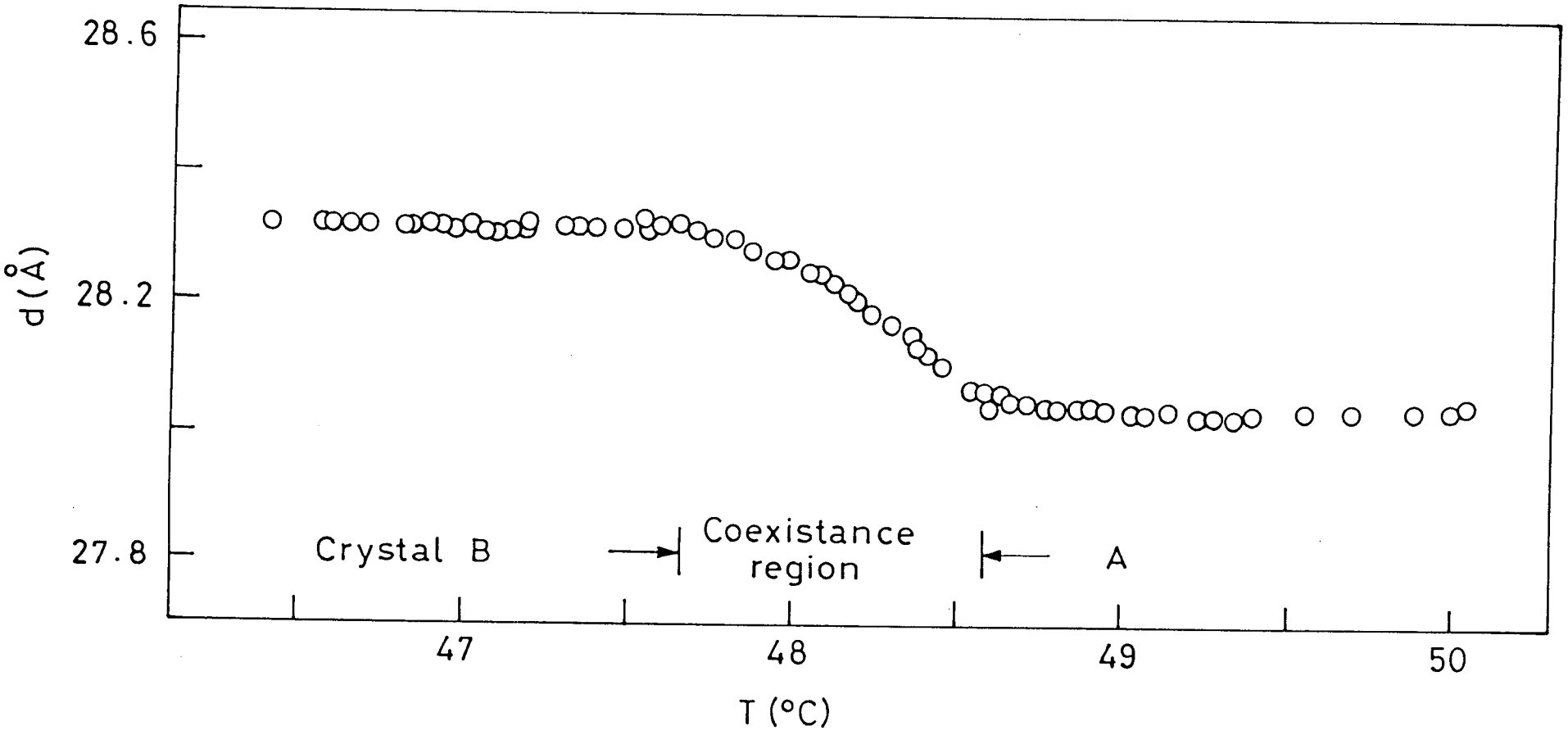

Figure 6.10

Variation of smectic layer spacing (d) in the neighbo hood of the B_{cryst} - A transition in 40.8 (Ref. 19).

order A-B_{cryst} transition and the second order A-B_{hex} transition show any differences in the dielectric dispersion. The typical loss curves of 40.8 in A and B_{cryst} phases as well as in co-existence region are shown in the Figure 6.11. It is interesting to see that the loss curves have sharp maxima in both A and B_{cryst} phases while in the co-existence region they are broad with a width of nearly double the width of the curves in A or B_{cryst} phase. This effect is similar to broadening of Xray diffraction peak in the two phase region due to the co-existence of two density modulations which was commented on earlier. Thus it is interesting to note that the dielectric dispersion could be a tool to probe the order of the transition provided, of course, the relaxation frequencies in the two phases are quite different. We shall discuss this aspect of the problem later. The representative loss curves in A and B_{hex} phases for 65OBC and 46OBC are shown in Figures 6.12 and 6.13. It is seen that these curves are sharp and not broadened for any temperature in A or B_{hex} phase of both 65OBC and 46OBC.

Figures 6.14-6.16 show Cole-Cole plots for a series of temperatures near the A-B transition for 40.8, 65OBC and 46OBC respectively. The values of f_R obtained from loss curves and Cole-Cole plots for the three compounds are listed in Tables 6.2-6.4. It is clear that in 40.8 the Cole-Cole plot is a perfect semicircle in the A (Fig.6.14a) and B_{cryst} (Fig. 6.14e) phases, signifying a single

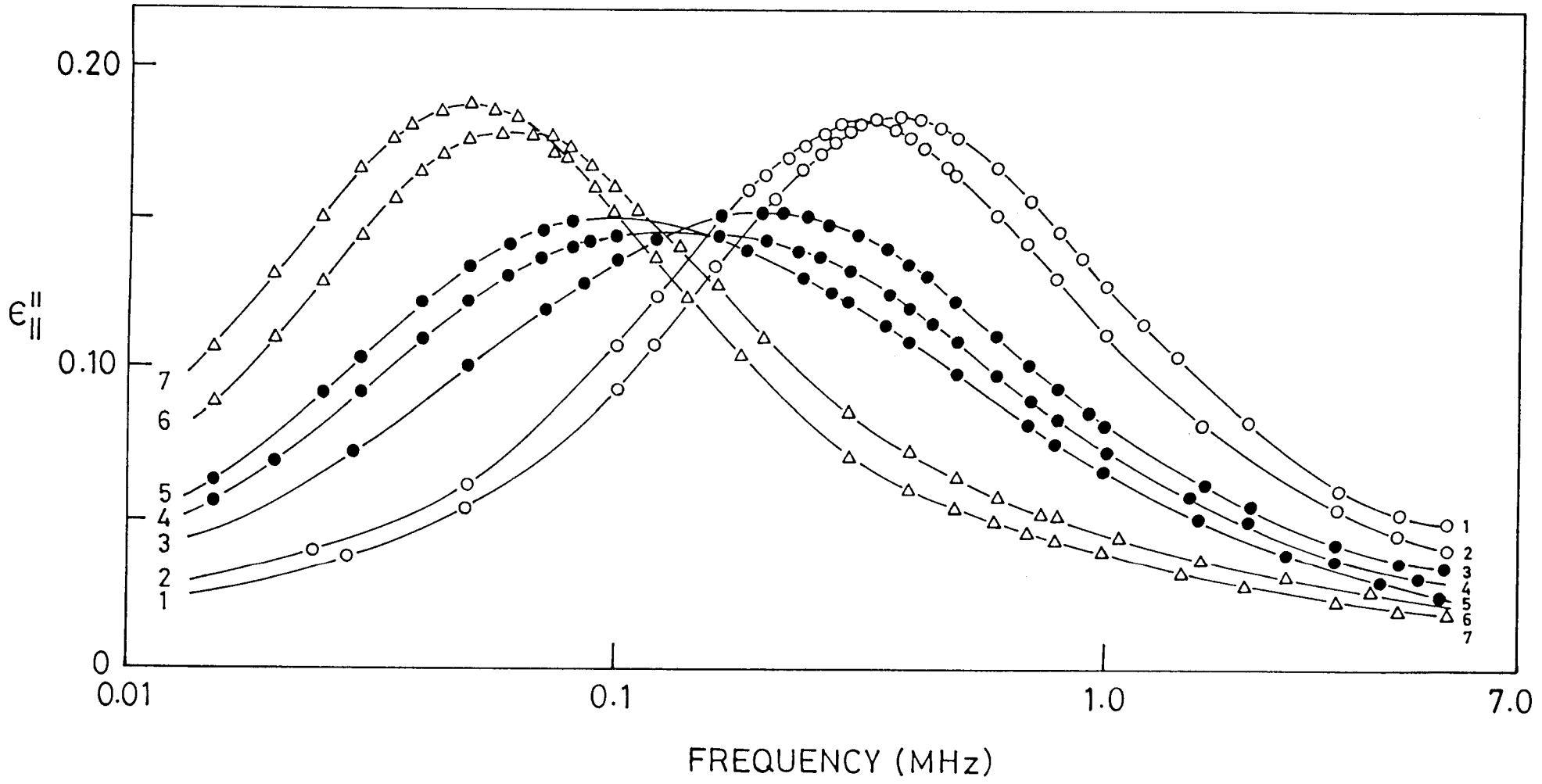

Figure 6.11

TCA representative loss curves at different temperatures in the vicinity of the A - B_{cryst} transition in 40.8. (a) A phase (O). (1) 51.5°C, (2) 49.65°C, (b) Two phase region (●). (3) 48.3°C, (4) 48.1°C, (5) 47.9°C. (c) B_{cryst} phase (Δ). (6) 46.45°C, (7) 44.3°C.

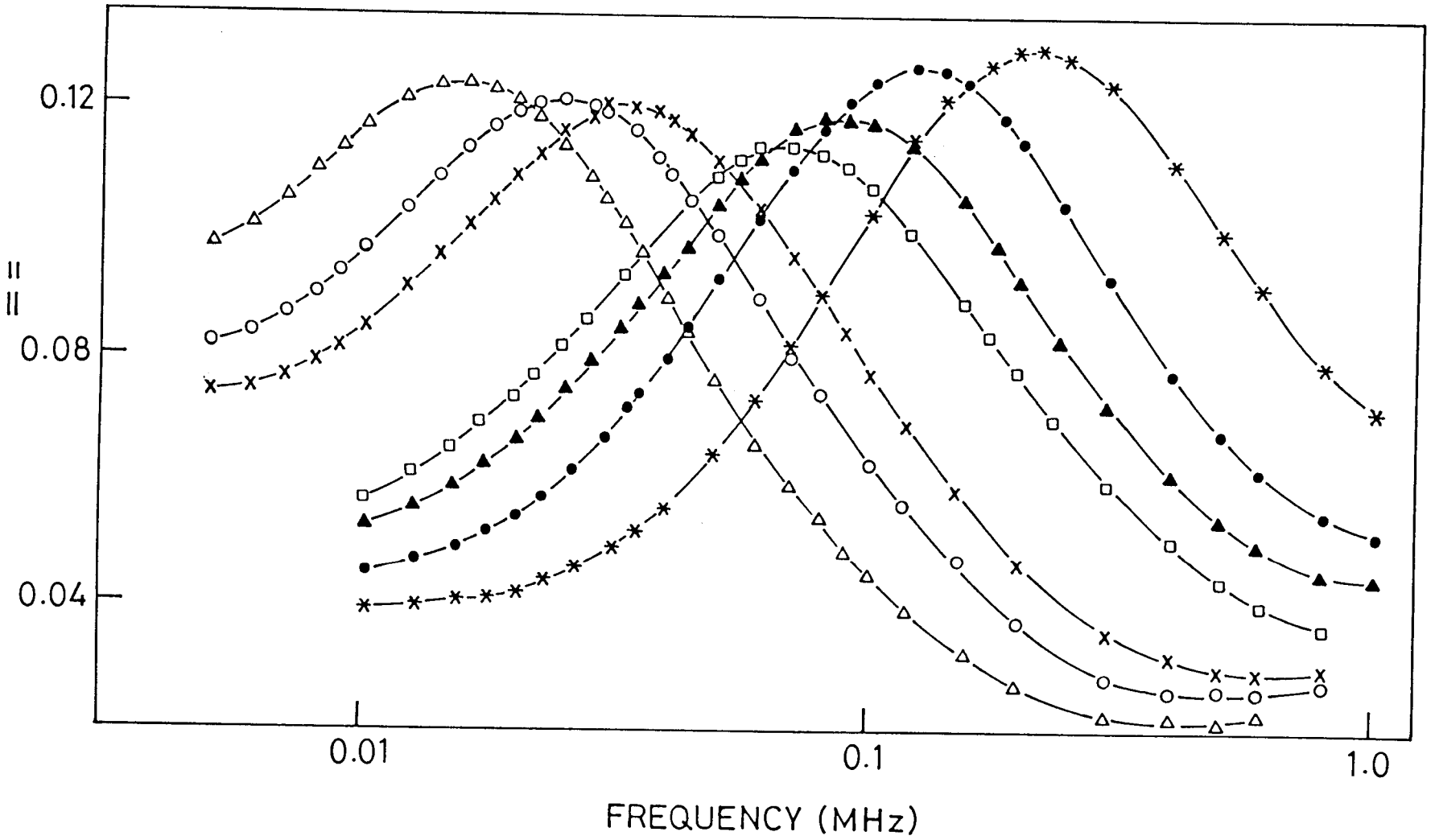

Figure 6.12

The representative loss curves of 650BC in the (a) smectic A (✱, 71.3°C; ● , 67.9°C; ▲ , 67°C) and (b) B_{hex} phase (□ 66.8°C, X 66.2°C, o 65.6°C and △ 64°C).

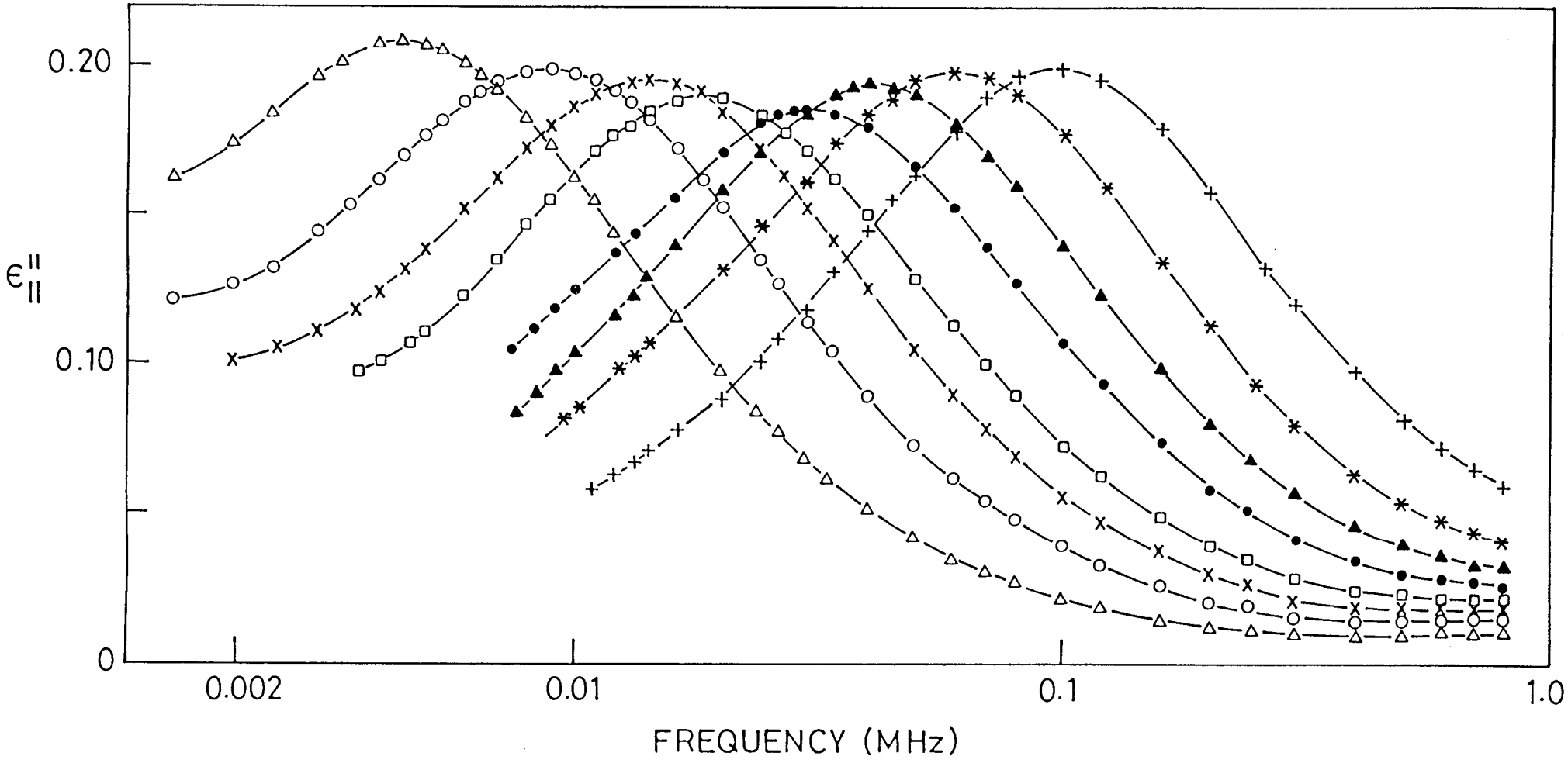

Figure 6.13

The representative loss curves of 4OOBC in the (a) smectic A (+, 71°C; *, 67.8°C) and (b) B_{hex} phase (▲, 66.6°C, ● 66.25°C, □ 66°C, × 65.8°C, O 64.9°C and △ 62.9°C).

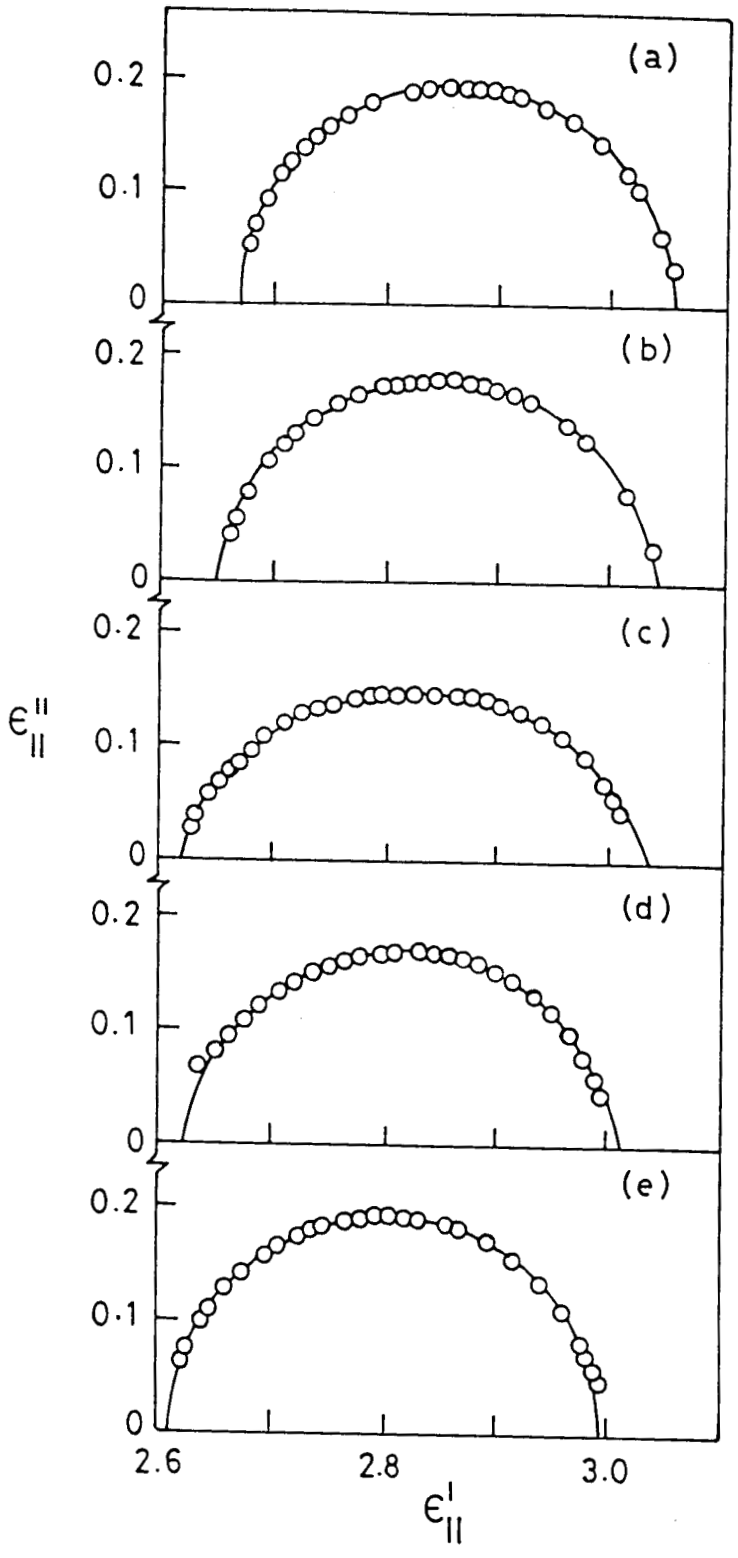

Figure 6.14

Cole–Cole plots at different temperatures in the vicinity of the B_{cryst} – Atransitioin in 40.8. (a) A phase, 51.5°C, (b)-(d) two phase region, 48.3, 48.1, 47.9°C respectively, (e) B_{cryst} phase, 44.3°C.

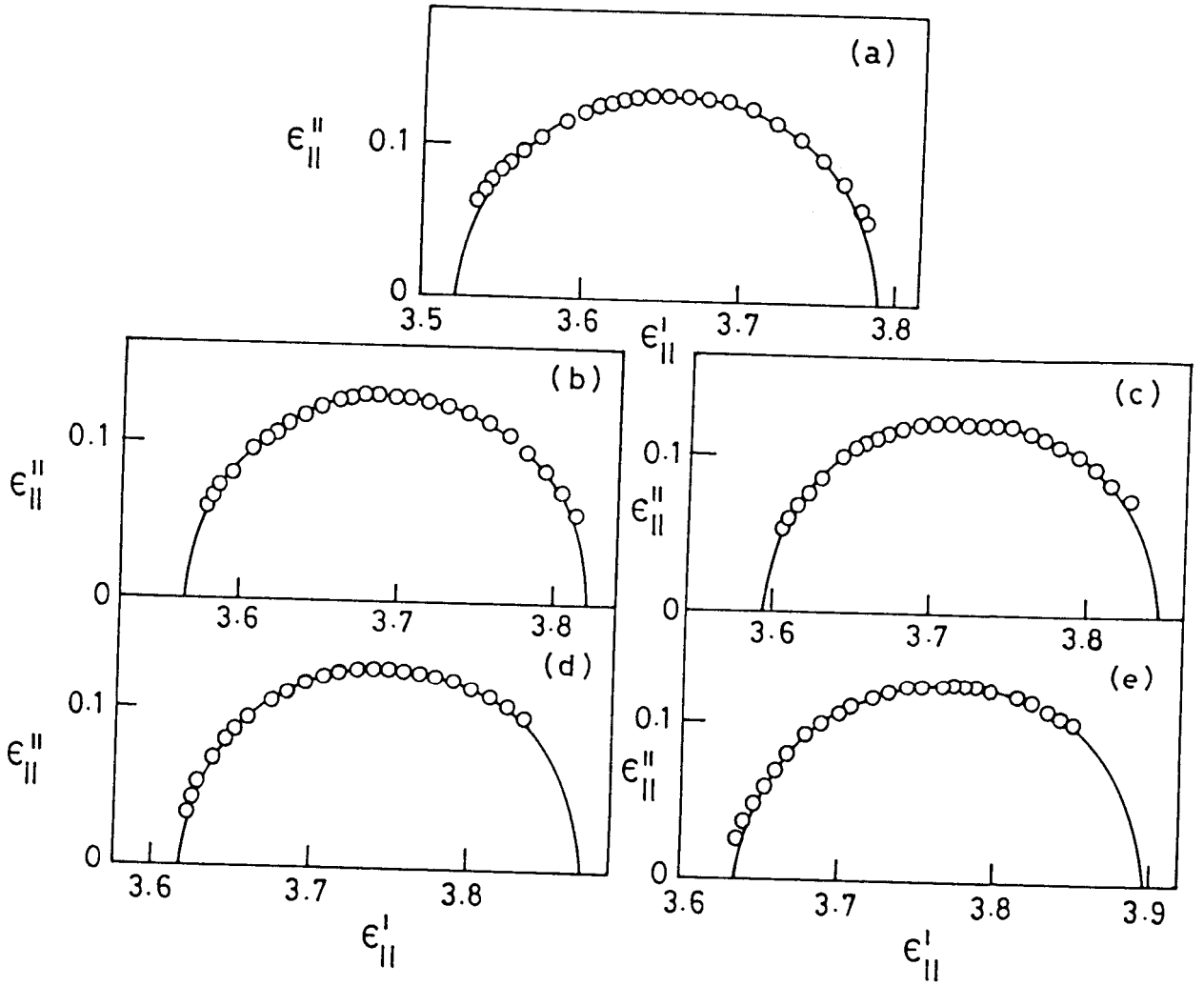

Figure 6.15

Cole-Cole plots at different temperatures in the vicinity of the B_{hex} - A transition in 650ÅC. (a) A phase, 71.3°C, (b) A phase, 67.9°C, (c)-(e) B_{hex} phase, 6≤.8, 65.6 and 64 °C respectively.

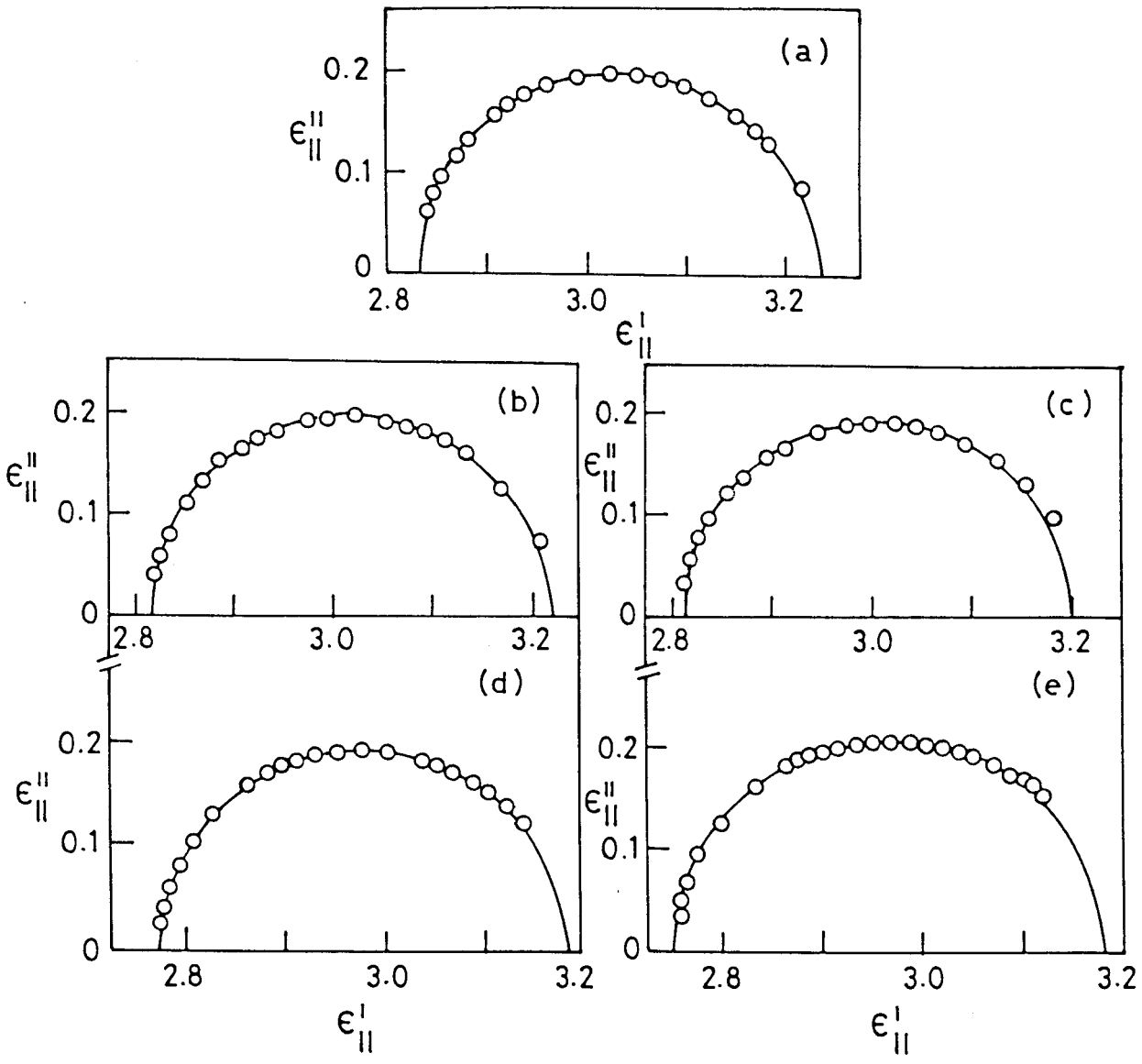

Figure 6.16

Cole–Cole plots at different temperatures in the vicinity of the B_{hex} – A transition in 4OBC. (a) A phase, 71°C, (b) A phase, 67.8°C, (c)-(e) B_{hex} phase, 66.6, 65.8 and 62.9°C respectively.

TABLE *6.2*

Frequency of relaxation f_R as a function of temperature in the smectic A, two phase region and smectic B_{cryst} phases of 40.8.

S.No.	Temperature (°C)	Frequency of relaxation (in MHz) From loss curve	From Cole-Cole	Mean f_R
		Smectic A		
1	62.45	1.1	1.07	1.085
2	62.05	1.05	1.01	1.03
3	59.95	0.840	0.838	0.839
4	58.1	0.700	0.705	0.703
5	54.8	0.520	0.525	0.523
6	53.85	0.480	0.482	0.481
7	53.35	0.460	0.455	0.458
8	53.1	0.450	0.443	0.447
9	52.55	0.430	0.425	0.428
10	52.2	0.415	0.414	0.415
11	51.95	0.410	0.404	0.407
12	51.75	0.400	0.395	0.398
13	51.5	0.385	0.386	0.386
14	51.25	0.375	0.373	0.374
15	50.95	0.365	0.366	0.366
16	50.6	0.350	0.349	0.350
17	50.25	0.340	0.338	0.339
18	49.95	0.330	0.329	0.330
19	49.65	0.315	0.314	0.315
20	49.4	0.308	0.304	0.306
		Two Phase Region		
21	49	0.285	0.272	0.279
22	48.75	0.260	0.244	0.252
23	48.5	0.247	0.215	0.231
24	48.25	0.200	0.179	0.190
25	48	0.135	0.0970	0.116
26	47.75	0.093	0.0774	0.0852
		B_{cryst} Phase		
27	47.5	0.079	0.0743	0.0767
28	47.25	0.072	0.0688	0.0704
29	47	0.068	0.0662	0.0671
30	46.7	0.064	0.0628	0.0634
31	46.45	0.062	0.0613	0.0616
32	46.0	0.058	0.0583	0.0582
33	45.5	0.056	0.0557	0.0558
34	44.3	0.050	0.0509	0.0505
35	41.7	0.041	0.0406	0.0408
36	38.9	0.033	0.0328	0.0329
37	36.4	0.027	0.0271	0.0270
38	34.85	0.024	0.0242	0.0241

TABLE *6.3*

Frequency of relaxation (f_R) as a function of temperature in the smectic A, B_{hex} phases of 65OBC

S.No.	Temperature (°C)	Frequency of relaxation (in MHz)		Mean f_R
		From loss curve	From Cole-Cole	
		Smectic A		
1	81.4	0.620	0.613	0.617
2	79	0.500	0.497	0.499
3	78.5	0.460	0.465	0.463
4	77	0.410	0.398	0.404
5	75.4	0.330	0.340	0.335
6	74.7	0.320	0.318	0.319
7	72.9	0.260	0.258	0.259
8	72.05	0.235	0.234	0.235
9	71.3	0.210	0.212	0.211
10	69.9	0.172	0.178	0.175
11	69.4	0.160	0.160	0.160
12	69.1	0.152	0.151	0.152
13	68.65	0.145	0.147	0.146
14	68.4	0.131	0.137	0.134
15	68.15	0.130	0.130	0.130
16	67.85	0.123	0.120	0.122
17	67.55	0.118	0.115	0.117
18	67.25	0.102	0.101	0.102
19	67	0.091	0.086	0.0885
		B_{hex} Phase		
20	66.75	0.065	0.0646	0.0648
21	66.4	0.037	0.0384	0.0377
22	66.2	0.033	0.0325	0.0328
23	65.9	0.0288	0.0287	0.0288
24	65.55	0.0245	0.0243	0.0244
25	65.2	0.022	0.0219	0.0220
26	64.85	0.0195	0.0194	0.0195
27	64.4	0.0175	0.0177	0.0176
28	64	0.015	0.0154	0.0152
29	63.25	0.0125	0.0128	0.0127
30	62.65	0.0113	0.0114	0.0114
31	62	0.0097	0.0103	0.01
32	61.1	0.0082	0.0085	0.0084

TABLE 64

Frequency of relaxation (f_R) as a function of temperature in the smectic A, B_{hex} phases of 4OBC

S.No.	Temperature (°C)	Frequency of relaxation (in MHz) From loss curve	From Cole-Cole	Mean f_R
		Smectic A		
1	86.85	0.490	0.492	0.491
2	84.3	0.353	0.354	0.355
3	82.6	0.320	0.323	0.322
4	80.9	0.260	0.264	0.262
5	79.6	0.235	0.240	0.238
6	77.35	0.180	0.183	0.182
7	75.6	0.155	0.157	0.156
8	74.7	0.132	0.137	0.135
9	72.6	0.107	0.108	0.108
10	71.7	0.098	0.0969	0.0975
11	71.2	0.093	0.0906	0.0918
12	70.7	0.086	0.085	0.0855
13	70.4	0.082	0.0807	0.0814
14	70.2	0.080	0.079	0.0795
15	70.0	0.078	0.0769	0.0775
16	69.7	0.075	0.0732	0.0741
17	69.45	0.072	0.0704	0.0712
18	69.15	0.0675	0.067	0.0673
19	68.8	0.064	0.0635	0.0638
20	68.45	0.0605	0.0602	0.0604
21	68.2	0.0570	0.0565	0.0568
22	67.95	0.0540	0.05330	0.0537
23	67.7	0.0500	0.0498	0.0499
24	67.5	0.048	0.0473	0.0477
25	67.25	0.04 10	0.0416	0.0413
26	66.95	0.03 10	0.0318	0.0314
		B_{hex} Phase		
27	66.7	0.0185	0.0189	0.0187
28	66.5	0.0143	0.0140	0.0142
29	66.25	0.0123	0.0123	0.0123
30	65.9	0.0100	0.0100	0.01
31	65.6	0.0089	0.0088	0.0089
32	65.2	0.0077	0.0078	0.0078
33	64.9	0.0071	0.00750	0.0073
34	64.7	0.0064	0.0064	0.0064
35	64.0	0.0050	0.0055	0.0053
36	63.55	0.0046	0.0046	0.0046
37	61.7	0.00290	0.0031	0.0030
38	59.95	0.0020	0.0021	0.0021
39	58.75	0.0015	0.0017	0.0016
40	57.6	0.0011	0.0013	0.0012

relaxation process. However, in the two phase region the plot is not a perfect semicircle (see Fig.6.14b-d), the distortion being maximum in the middle of the co-existence region. This is due to the superposition of two relaxation frequencies corresponding to the A and B regions. This effect is similar to the averaging of the layer spacing in the two phase region mentioned earlier. On the other hand it was found that for both 650BC and 460BC, the Cole-Cole plot was a perfect semicircle for all temperatures. Representative Cole-Cole plots for 650BC and 460BC (shown in Figures 6.15 and 6.16) clearly illustrate this. Thus a careful scrutiny of the Cole-Cole plots at temperatures in the close vicinity of the transition shows the difference between the first order $A-B_{cryst}$ and the second order $A-B_{hex}$ transitions.

f_R vs. $1/T$ plots in the A and B phases of the three compounds are shown in Figures 6.17 - 6.19. The activation energies (W) in the A and B phases, evaluated from the linear portions of the plots are listed in the table 6.5. Several interesting features are clear from these diagrams; (i) There is a drastic decrease in f_R (by about a .factor of four) on going over from the A to the B phase in all the three compounds. (ii) For 40.8 the variation of f_R is linear in the A and B_{cryst} phases almost up to the transition temperature (Fig.6.17). In the case of 650BC and 460BC, f_R shows marked pre-transitional variations in both A and B_{hex} phases, the effect

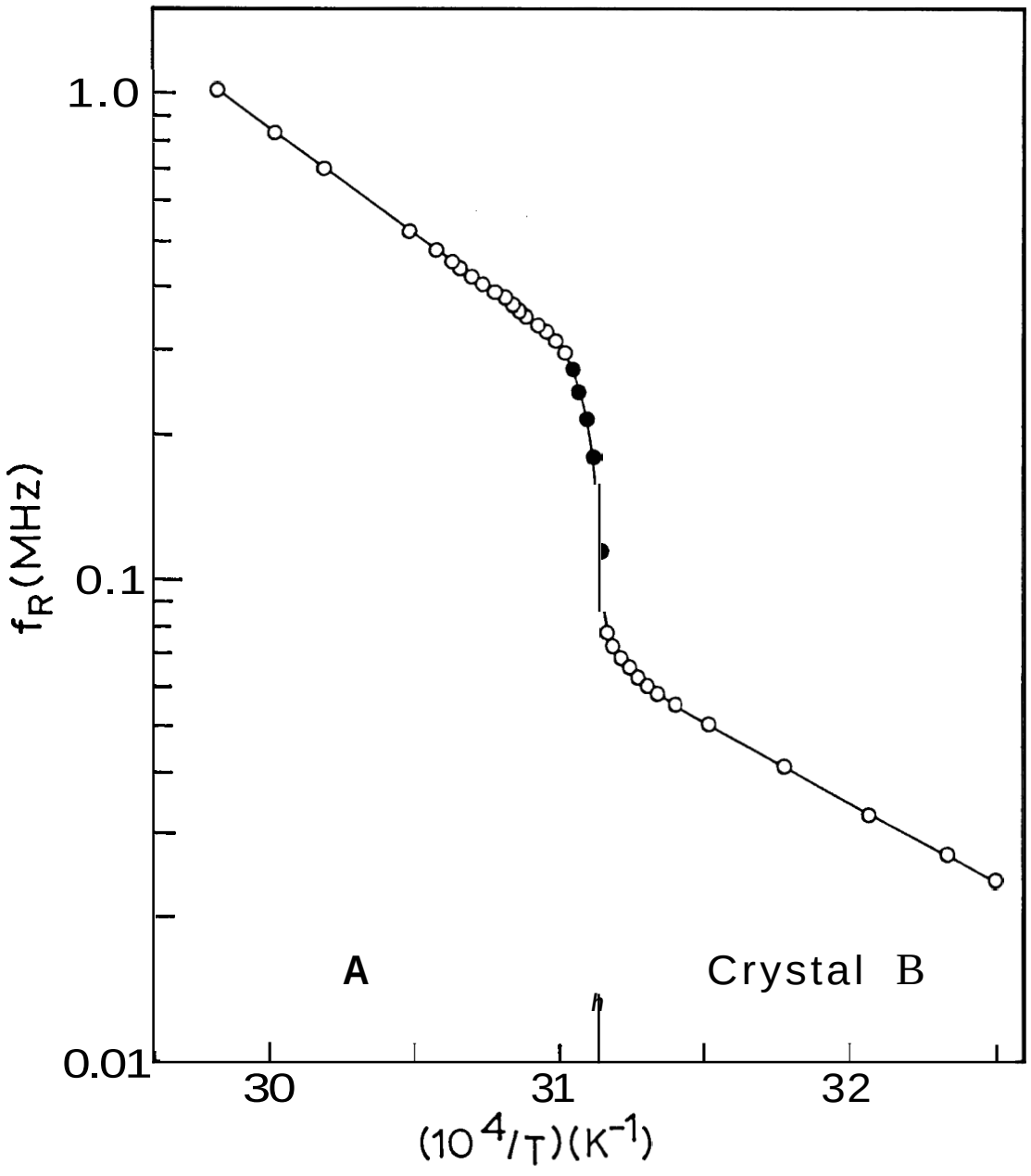

Figure 6.17

Plot of f_R, the low frequency relaxation of $\varepsilon_{||}$ versus 1/T in the A and $B_{crystal}$ phases of 40.8. The solid circles denote the temperatures (in the two-phase region) for which the Cole-Cole plots are distorted (see Fig. 6.14).

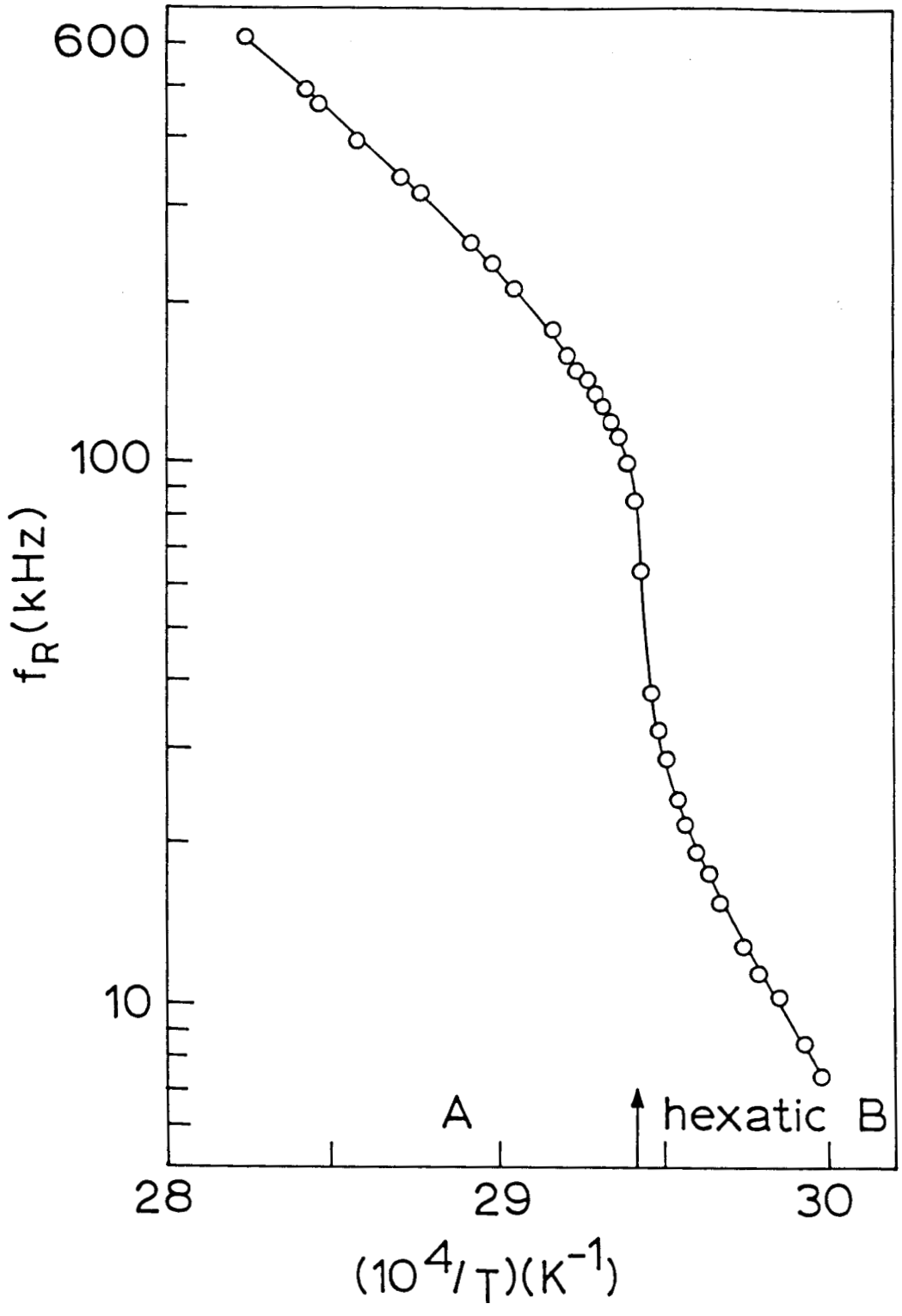

Figure 6.18

Plot of f_R versus 1/T in the A and B_{hex} pnases of 650BC.

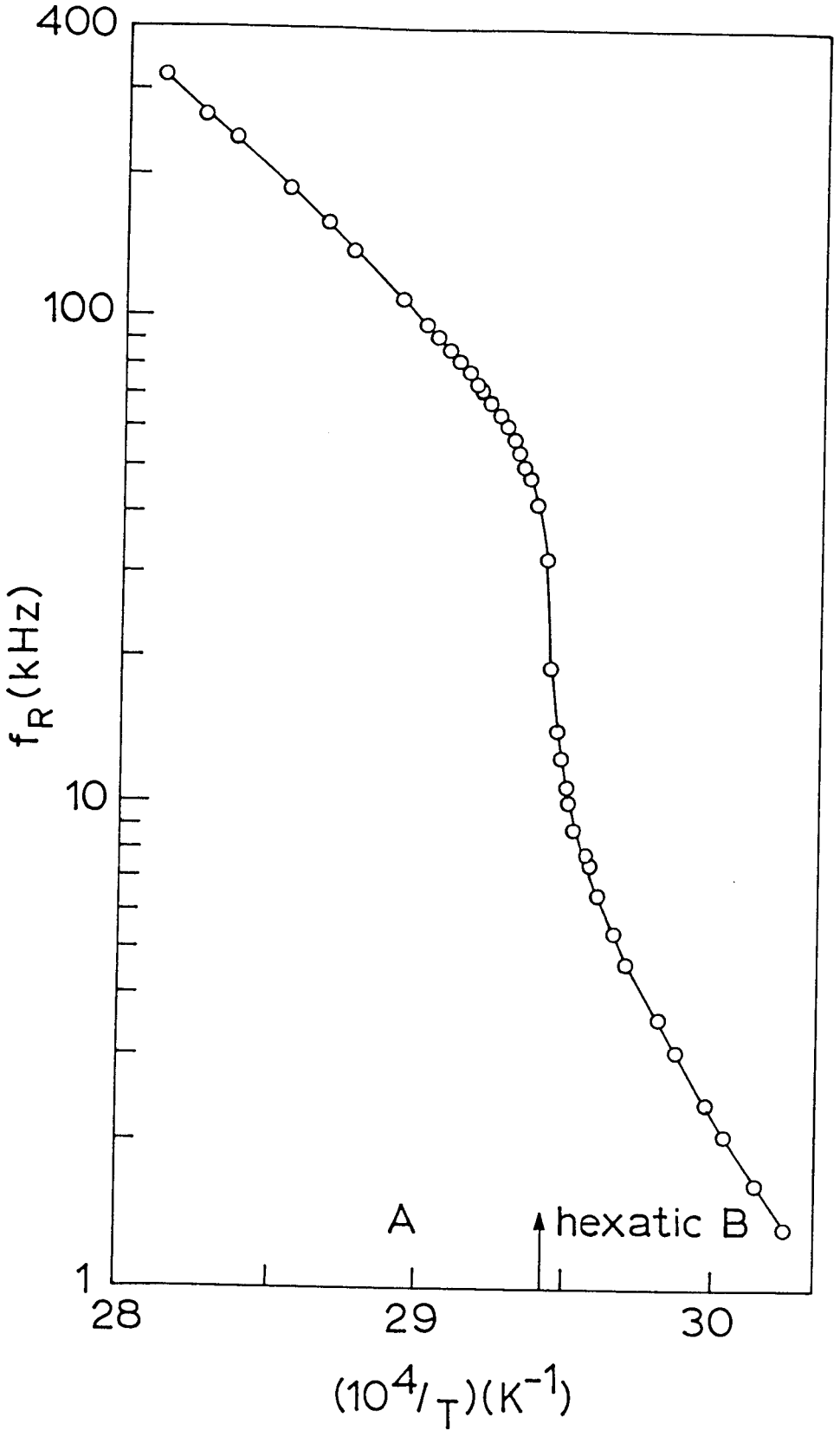

Figure 6.19

Plot of f_R versus 1/T in the A and B_{hex} phases of 460BC

TABLE *6.5*

Activation energy (W) in the srnectic A and B phases of 40.8, 65OBC and 46OBC

S.No.	Compound	Activation energy (in eV)	
1	4O.8	Srnectic A	Srnectic BCryst
		0.85	0.66
2	65OBC	Srnectic A	Srnectic B_{hex}
		1.09	2.05
3	46OBC	Srnectic A	Srnectic B_{hex}
		1.13	2.0 1

being more pronounced in the B_{hex} phases (Figures 6.18 & 6.19). (iii) the value of W in the B_{cryst} phase of 40.8 is less than that in the A phase whereas in the case of both 65OBC and 46OBC $W_{B_{hex}} > W_A$. (Here $W_{B_{hex}}$ is taken for temperatures farthest from A - B_{hex} transition temperature).

There are some earlier reports[20-23] on the dielectric relaxation studies of compounds exhibiting the B phase. In all these cases a jump in f_R at the A-B transition has been observed. This has been attributed to three factors, viz., (1) the increased two-dimensional ordering of the centres of molecules within the smectic B layers leading to a greater hindrance to the reorientation of the long molecular axis compared to the A phase,[20,21] (2) the first order nature of the A-B transition,[22] and (3) the appearance of a collective libration in the two-dimensional hexagonal layer.[21] We now know from high resolution Xray scattering studies[1,5] that in-plane positional ordering of the molecules in the layer is widely different for the B_{cryst} and B_{hex} phases. As mentioned earlier, we also know from high resolution ac calorimetric studies[8] that the A-B_{cryst} transition in 40.8 is first order while the A-B_{hex} transition in 65OBC and 46OBC is second order. Despite these differences, a jump in f_R of about the same magnitude is seen by us for both A-B_{cryst} and A-B_{hex} transitions. This could perhaps be due to the existence of long-range bond-orientational order

in both B_{cryst} and B_{hex} phases, this being absent in the A phase.

In conclusion our studies show that although essentially the same behaviour in A and f_R is seen at both the A-B_{cryst} and A-B_{hex} transitions the activation energy in the B_{cryst} phase is less than that in the A phase while the opposite is the case for the B_{hex} phase. The exact correlation between the structural differences of the B_{cryst} and B_{hex} phases and the differences in their dielectric behaviour is still an open question.

REFERENCES

1 P.S.Pershan, G.Aeppli, J.D.Litster and R.J.Birgeneau, Mol. Cryst. Liq. Cryst., 67, 205 (1981)

2 A.J.Leadbetter, J.C.Frost, and M.A.Mazid, J. Phys. Lett. (Paris), 40, 325 (1979).

3 B.I.Halperin and D.R.Nelson, Phys. Rev.Lett., 41, 121 (1978).

4 R.J.Birgeneau and J.D.Litster, J.Phys.Lett. (Paris), 39, 399 (1978)

5 R.Pindak, D.E.Moncton, S.C.Davey and J.W.Goodby, Phys. Rev. Lett., ***46***, 1135 (1981).

6 C.C.Huang, J.M.Viner, R.Pindak and J.W.Goodby, Phys. Rev. Lett., 46, 1289 (1981).

7 J.M.Viner, D.Lamey, C.C.Huang, R.Pindak and J.W.Goodby, Phys.Rev., A28, 2433 (1983)

8 T.Pitchford, G.Nounesis, S.Dumrongrattana, J.M.Viner, C.C. Huang and J.W.Goodby, Phys. Rev., A32, 1938 (1985).

9 R.Mahmood, M.Lewis, R.Biggers, V.Surendranath, D.Johnson and M.E.Neubert, Phys. Rev., A33, 519 (1986).

10 G.Nounesis, C.C.Huang and J.W.Goodby, Phys. Rev. Lett., 56, 1712 (1986).

11 S.C.Davey, J.Budai, J.W.Goodby, R.Pindak and D.E.Moncton, Phys. Rev. Lett., 53, 2129 (1984).

12 C.Rosenblatt and J.T.Ho, Phys.Rev., A26, 2293 (1982).

13 R.Pindak, W.O.Sprenger, D.J.Bishop, D.D.Osheroff, and J.W. Goodby, Phys.Rev.Lett., 48, 173 (1982).

14 G.Poeti, E.Fanelli and D.Guillon, Mol. Cryst.Liq. Cryst., 82, 107 (1982).

15 R.Bruinsma and G.Aeppli, Phys.Rev.Lett., 48, 1625 (1982).

16 A.M.Levelut, R.J.Tarento, F.Hardouin, M.F.Achard and G.Sigaud, Phys.Rev., A24, 2180 (1981).

17 F.Hardouin, A.M.Levelut, M.F.Achard, G.Sigaud, J. Chim. Phys., 80, 53 (1983).

18 J. W.Goodby and R.Pindak, Mol. Cryst.Liq. Cryst., 75, 233 (1981).

19 Geetha G. Nair (unpublished); see also C.Nagabhushan, Geetha G.Nair, B.R.Ratna, R.Shashidhar and J.W.Goodby,Liquid Crystals (in press)

20 A.Buka, L.Bata and H.Kresse, Hungarian Academy of Sciences Report, KFKI-1980-04.

21 L.Bata and A.Buka, Mol. Cryst.Liq.Cryst., 63, 307 (1981).

22 A.Buka, L.Bata, K.Pinter and J.Szabon, Mol. Cryst.Liq.Cryst. Lett., 72, 285 (1982).

23 L. Benguigui, Phys. Rev., A28, 1852 (1983).